Langmuir

Article

pubs.acs.org/Langmuir

Molecular Dynamics Investigation on Adsorption Layer of Alcohols at the Air/Brine Interface

Cuong V. Nguyen,[†] Chi M. Phan,*[,†] Ha M. Ang,[†] Hiromichi Nakahara,[‡] Osamu Shibata,[‡] and Yoshikiyo Moroi[‡]

[†]Department of Chemical Engineering, Curtin University, Perth WA 6845, Australia

[‡]Department of Biophysical Chemistry, Faculty of Pharmaceutical Sciences, Nagasaki International University, Sasebo, Nagasaki 859-3298, Japan

ABSTRACT: Alcohols are a significant group of surfactants which have been employed extensively in industry to improve the interfacial effects. Recently, the change in surface potential (ΔV) of two isomeric hexanols, methyl isobutyl carbinol (MIBC) and 1-hexanol, was investigated by using an ionizing ^{241}Am electrode. It clearly showed the opposite effects between MIBC and 1-hexanol in the interfacial zone: one enhanced the presence of cations, whereas the other enhanced the presence of anions. This study employs molecular dynamics simulation to provide new insights into the interactions between alcohol molecules and ions as well as water at the molecular level. The results qualitatively agreed with the experimental data and verified the significance of MIBC branching structure on the molecular arrangement within the interfacial zone. The results also highlighted the role of the second water layer on the interfacial properties.

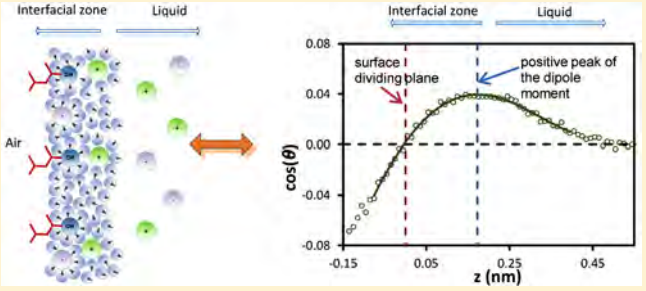

INTRODUCTION

Because of the amphiphilic structure and high solubility, alcohols form an important class of surfactants that are widely utilized in industrial processes.[1,2] Alcohols adsorbed at the air/water interface[3] can significantly stabilize foams for mineral flotation. In spite of the applications, the influences of alcohol structure on the process efficiency remain poorly understood. The deficits in the knowledge limit the capacity of chemical design for the industrial processes.

One of the quantifiable properties of the interface is the surface potential (ΔV) change,[4] which is a prominent factor for thin film stabilizing, foaminess, double-layer charge, and disjoining pressure.[5] The effect of surfactant structure on surface potential can be very significant. For instance, the change in hydrocarbon tails between cetyltrimethylammonium bromide (CTAB) and tetradecyltrimethyl bromide (TTAB) can dramatically alter the surface potential:[6] while the surface potential for TTAB remains constant at 0 mV, the surface potential of CTAB solution steeply increases 420 mV. Similarly, alcohols can significantly increase surface potential by reorienting/disrupting water molecules.[6,7]

Recently, we have quantified the influence of two isomeric alcohols on the air/water interfacial potential.[8,9] These alcohols, methyl isobutyl carbinol (MIBC) and 1-hexanol, are the prominent frothers for the mineral flotation process.[10,11] Notably, the modeling results showed contrast behaviors between MIBC and 1-hexanol: the presence of cations is enhanced by adsorbed MIBC, whereas the presence of anions is enhanced by adsorbed 1-hexanol. The difference might be the underpinning mechanism for the superior performance of MIBC in mineral froth flotation. In particular, the enhanced cations might increase the selectivity of mineral particles and increase the efficiency of the flotation. We hypothesized that the branching structure of MIBC plays a critical role in the phenomena.

Atomistic simulation is the most effective tool to quantify the molecular structure on the macro properties.[12−15] In this study, the adsorption layers were investigated by molecular dynamics using the available models. The variation of surface tension and surface potential of 1-hexanol and MIBC solutions were calculated and compared to experimental results. The arrangement and interaction between molecules were also studied to provide important insights into the interfacial zone.

EXPERIMENT

Surface Tension Measurement. The experimental setup consisted of Wilhelmy plate method,[16] using a tensiometer KSV Sigma 701 (KSV Instrument Ltd., Finland) cooperated with an automatic microdisperser. The Wilhelmy plate is made of platinum with the perimeter of 39.4 mm. All experiments were measured at the temperature of 298 K.

Surface Potential (ΔV) Measurement. The surface potential of the solutions was measured relative to the pure supporting electrolyte potential using an ionizing ^{241}Am electrode. The description of surface potential measurement can be found elsewhere.

Received: August 8, 2014
Published: December 15, 2014

DOI: 10.1021/la504471q
Langmuir 2015, 31, 50−56

COMPUTATIONAL METHOD

The vacuum−water interface was simulated using the simulation box constructed with a slab of water layer (around 10 nm thickness) placed between two empty regions (10 nm each) as shown in Figure 1c.

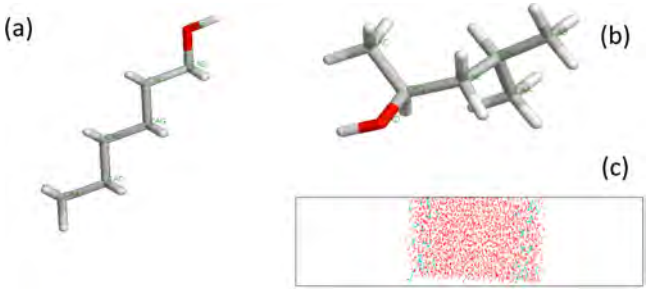

Figure 1. Simulation setup: (a) 1-hexanol, (b) MIBC, and (c) simulation box (red: water; blue: MIBC).

The GROMACS version 4.5.5[17] was used to generate the molecular trajectories using a time step of 1 fs. In this study, a popular water potential, SPC/E,[12] was employed. The molecular potentials for MIBC and ions (Na^+ and Cl^-) have been described by the GROMOS96 force field.[18−20] The charge distribution of the hydroxyl group (Table 1) was selected from the proposed distribution in the literature,[21] which has been successfully used for the 1-hexanol/water interface.[22] All hydrogen atoms, except H in the hydroxyl group, were united with the corresponding carbon. The α-carbon has a positive charge (0.265), whereas all other carbons have a neutral charge.

Table 1. Charge Distributions for MIBC, 1-Hexanol, and Ions

united atom/ions	charge	united atom/ions	charge
CH_x	0	H	0.435
Cα (−OH)	0.265	Na^+	1
O	−0.700	Cl^-	−1

Different numbers (2, 4, 6, 8, 10, 12, 14, 16, and 18) of alcohols were placed at both sides of two interfaces before filling up the cell with water. Subsequently, 214 water molecules were replaced by 107 Na^+ and 107 Cl^- ions, which correspond to a concentration of 2 M. A simulation without alcohols, that is NaCl in water, was also performed to provide a reference system.

The first simulation step was performed at constant temperature and pressure (298 K and 1 bar) in an orthorhombic simulation cell of 3 nm × 3 nm × 10 nm, using a Berendsen barostat[23] with a relaxation time of 2 ps and cutoff of 1.3 nm. The x- and y-dimensions of the box were adjusted correspondingly. Consequently, the z-length was increased to 30 nm to create two empty regions (as shown in Figure 1c).[12] The methodology has been widely employed to simulate the air/water interface.[24] Detailed discussion and justification of the method have been reviewed in the literature.[25]

The simulation was then performed for 20 ns in constant temperature (298 K) and volume using a Nosé−Hoover thermostat. The last 10 ns was used for density, surface potential, and water dipole moment analysis. The geometry of the water molecules and bond lengths of MIBC molecules were kept unchanged by means of LINCS[26] algorithms. Ewald[27] sums were used to deal with the electrostatic interactions. The surface tension, distributions of alcohols, water, and ions, and surface potential were obtained by analyzing the trajectories recorded at every 500 fs.[28]

RESULTS AND DISCUSSION

Density Distribution. The average density distribution was calculated for water, either MIBC or 1-hexanol, Na^+, and Cl^-. From Figure 2, it can be seen that alcohols are clearly distributed around the air−water interface, and there was no interaction between alcohols from the two opposite sides. The densities of Na^+ and Cl^- near the air/water interface are smaller than that in bulk, which is consistent with the negative adsorption (i.e., the air/water interfaces expel inorganic ions).

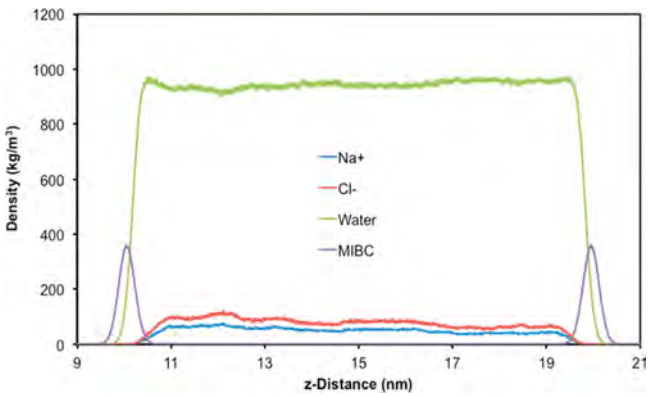

Figure 2. Density distribution of simulation box with eight MIBCs on each side.

The density distribution of water, $\rho(z)$, was determined by fitting simulation data with an error function of the following form (with the assumption that the vapor density equal to zero):[29]

$$\rho(z) = \frac{\rho_0}{2}\left(1 - \mathrm{erf}\left(\frac{z - z_0}{\sqrt{2w}}\right)\right) \quad (1)$$

where ρ_0 is the water density, z_0 is the location of the Gibbs dividing plane (GDP), and w is a parameter related to the width of the interface.[13]

It has been found that water density in NVT simulation was less than 0.05% of water density before the extension of simulation box. In other words, the simulated water layer represents water at 1 bar. The average density distributions for hydrophobic tail (carbon chain) and hydrophilic head (hydroxyl) were calculated separately. In this study, the "head" is defined as the −OH group and the "tail" consists of the whole carbon chain.

The density profiles of the head and tail groups were fitted using the Gaussian distribution:

$$\rho_i = \rho_i^0 \exp\left[\frac{-4(z - z_i^0)^2}{\sigma_i^2}\right] \quad (2)$$

where i is either t (tail) or h (head), σ_i is the width of the distribution, z_i^0 is the center, and ρ_i^0 is the density at center.

In Figure 3, the dividing plane was located where water interface excess equals zero. For all concentrations, the carbon

DOI: 10.1021/la504471q
Langmuir 2015, 31, 50−56

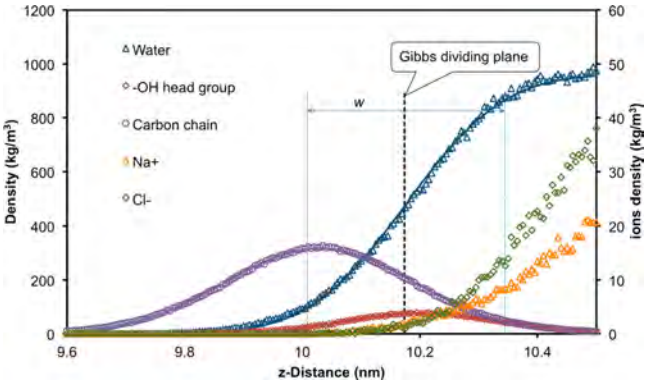

Figure 3. Density of water, hydrophobic tail, and hydrophilic head (eight MIBCs on each side). Best-fitted (solid lines).

chains are mostly located outside the Gibbs dividing plane. On contrast, the −OH groups are located further inside the liquid phase. Hence, the alcohols expectedly behaved as a surfactant.

Surface Tension. The surface tension $\gamma(t)$ was calculated from the pressure tensor:

$$\gamma(t) = \frac{1}{2}\int_0^{L_z}\left\{P_{zz}(z,t) - \frac{P_{xx}(z,t) + P_{yy}(z,t)}{2}\right\}\mathrm{d}z \tag{3}$$

where L_z is the length of the box and P_{xx}, P_{yy}, and P_{zz} are the three diagonal components of the pressure tensor along the x-, y-, and z-direction, respectively.

Subsequently, an accumulated average of surface tension was obtained for each simulation. In this study, the pure water surface tension was calculated at 59.2 mN/m, which is similar to literature values: 61.9,[12] 63.6,[30] and 60.7 mN/m.[13] These values are ∼12 mN/m less than the experimental γ at 72 mN/m. In the presence of 2 M NaCl, our simulation increased γ to 60.5 mN/m, which was consistent with the experimental trend.

Since the simulated γ of pure solvent does not match the experimental data, the influence of solutes/surfactant is often compared in term of the surface tension reduction.[19] In other words, the simulated data are adjusted by $\Delta\gamma_0$, which is the difference between simulated and experimental surface tension of the reference system. For our systems, $\Delta\gamma_0$ equals 14.8 mN/m. The theoretical surface tension in Figure 4 was generated from the previous experimental studies[8,9,11] and used to compared to simulated results for alcohol solutions.

In Figure 4a, it can be seen that the simulated γ decreased with increasing MIBCs and followed the experimental data qualitatively. On contrast, the simulated γ of 1-hexanol remained almost constant over the concentration range. The variation in simulated surface tension can be contributed to water models, simulation size (box dimension), running time, and cutoff radius. The influences of these factors are being discussed in the literature.[12−15] In the presence of surfactants, the simulated γ also fluctuated up to ±3 mN/m.[31,32]

Surface Potential. The surface potential was obtained for the production run using the formula

$$\psi(z) - \psi(0) = -\int_0^z \mathrm{d}z' \int_0^{z'} \frac{\rho_e(z')}{\varepsilon_0}\,\mathrm{d}z'' \tag{4}$$

where ε_0 is the vacuum permittivity, ψ is electric potential, and ρ_e is the charge density.

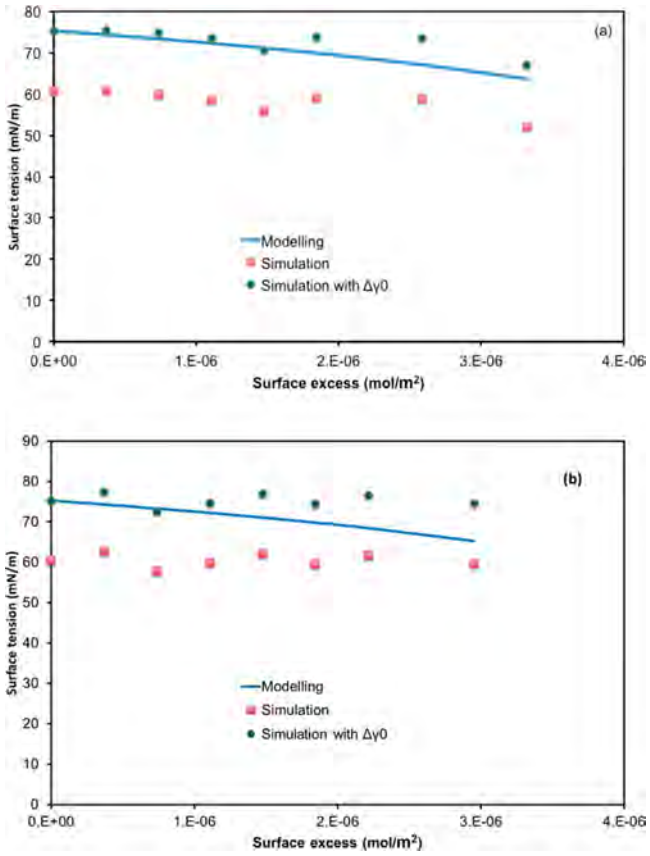

Figure 4. Equilibrium surface tension as a function of (a) MIBC and (b) 1-hexanol excess in 2 M NaCl.

The reference system had a negative potential at −578 mV, which was consistent with the literature value for pure water, −546 mV.[33] It is noteworthy that inside the liquid phase the potential changes insignificantly due to the random orientation of water molecules.

The potentials of alcohols and combined ions/water were obtained separately. Figure 5 shows that alcohols generate a negative potential at the interface. This is expected from the charge distribution between the α-carbon and oxygen in Table 1. However, alcohols increased the potential of ions/water, i.e.,

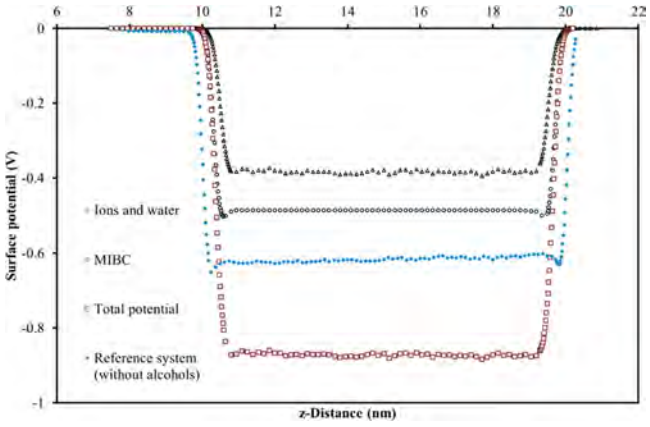

Figure 5. Surface potential distribution along the z-axis: with 20 MIBCs on each side. The potential of MIBC system was separated into two components: MIBCs and the rest (ions plus water). The potential of a reference system (2 M NaCl in water) is also included.

DOI: 10.1021/la504471q
Langmuir 2015, 31, 50−56

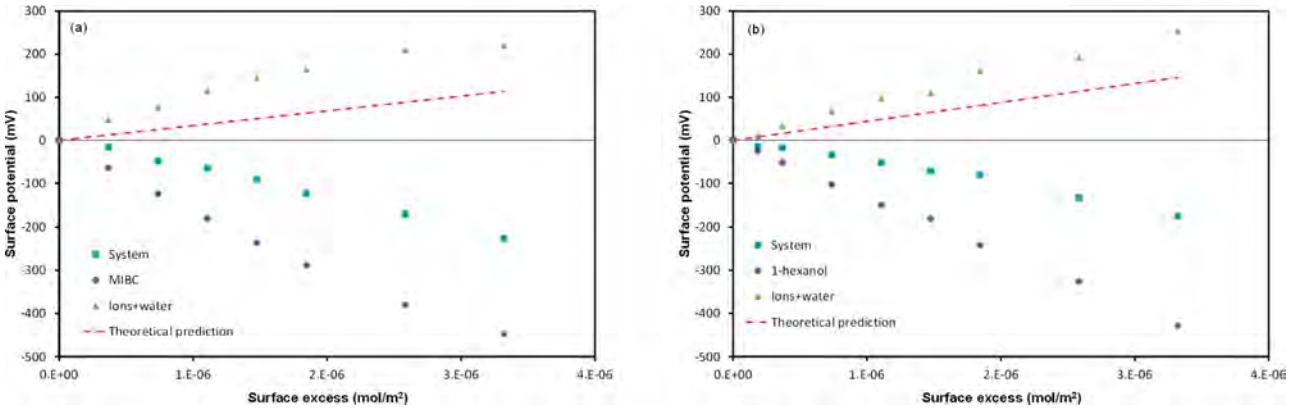

Figure 6. Surface potential as a function of MIBC (a) or 1-hexanol (b) surface excess, with reference potential was taken at 2 M NaCl solution.

less negative in comparison to the reference system. This effect demonstrates the disorientation of water molecules/displacement of ions by the adsorbed alcohols as proposed theoretically.[8] On the other hand, the net change in surface potential was decreased.

Figure 6 shows simulated versus the theoretical potentials. The water/ions potential increased with increasing alcohol concentrations and qualitatively agreed with theoretical data. On the other hand, the total potential was decreased. One of the reasons for this discrepancy is the oversimplification of alcohol charge distribution. For instance, the hydrocarbon chain of alcohols could have more complicated charge, and some carbon−carbon bonds may contribute positively on the overall potential. Summarily, the results indicated that the reorientation of water molecules, due to the presence of alcohols, increased the surface potential as observed experimentally.

Arrangement of Water Molecules at the Interface. Since the ion densities (Figure 2) cannot distinguish cation/anion distribution, the structure of the interfacial layer was analyzed. The water orientation in the interface region was quantified by the water dipole order parameter, $\cos(\theta)$, in which θ is the angle between the positive z-axis and the water dipole.

The simulation with NaCl in water (i.e., without MIBCs or 1-hexanol) indicated a well-structured arrangement of the interface zone with different layers of water molecules. Water molecules near the interface have two distinctive orientations: one points to the vapor side and the other points to liquid phase. The second layer is characterized by the positive peak of $\cos(\theta)$. The two-layer structure has also been reported in the literature.[13,34] Further inside the bulk, the average angle is zero as water is randomly oriented. Consequently, there is a gradual decrease from the second layer (the positive peak) to the bulk.

The presence of alcohols, either MIBCs or 1-hexanol, disrupted the interfacial arrangement as demonstrated in Figure 7. The positive peak remained evidenced but was shifted further outside with the increasing alcohols concentration. At high concentrations, the values of $\cos(\theta)$ were positive throughout the interfacial zone. In these instances, all water molecules at the outmost layer were reoriented (pointing to the liquid side) to comfort alcohol molecules. Consequently, it is conceivable that the positive peak corresponds to a boundary between the bulk and the interfacial zone.

Distribution of Ions within the Interfacial Zone. As described in experimental studies,[8,9] the relative amounts of

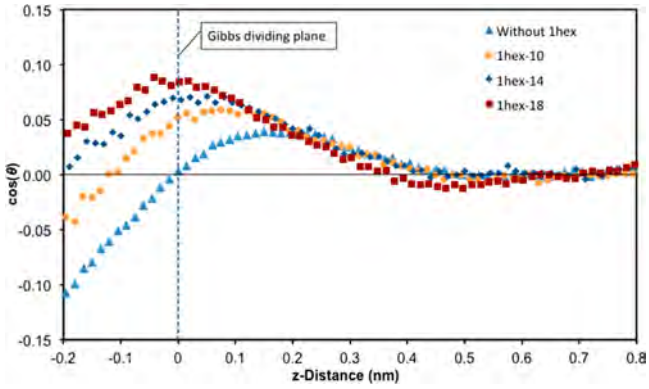

Figure 7. Profiles of water dipole order parameter, $\cos(\theta)$, with different 1-hexanol concentrations. The data of four simulations were shifted horizontally so that the Gibbs dividing plane was located at z = 0.

Na^+ and Cl^- within Stern layer were reversed between 1-hexanol and MIBC. Theoretically, the limit of Stern layer is a boundary between (i) the bulk in which ions follow Brownian motion and (ii) the interfacial zone within which the ions movement are constrained by the asymmetric molecular arrangement. However, quantifying this boundary from the ion densities is not practical. It should be highlighted that the usage of the Gibbs dividing plane is not appropriate for this purpose since the ionic interactions with the −OH group will be mainly inside the liquid phase. In the literature, there is no proposed method to quantify the location of this boundary, which is the limit of the interfacial zone.

In this study, we hypothesize that the limit of the interfacial zone corresponds to the peak of the water dipole order, i.e., the center of the second water layer. The underlying argument is that on the right of the peak the water molecules are constrained by the interfacial arrangement. On the left of the peak, water molecules start moving randomly as dictated by the bulk phenomena. The exact location of the peak was found by fitting a polynomial function (Figure 8) to the dipole order profile.

Consequently, the numbers of ions within interfacial layer were calculated based on the accumulative number densities of Na^+ and Cl^-, that is, the total ions from the vapor phase to the position of the peak (Figure 9a,b).

It can be seen from Figure 9a that the number of Cl^- inside the interfacial layer was always less than the number of Na^+ within this zone. However, the alcohols reduced the available

DOI: 10.1021/la504471q
Langmuir 2015, 31, 50−56

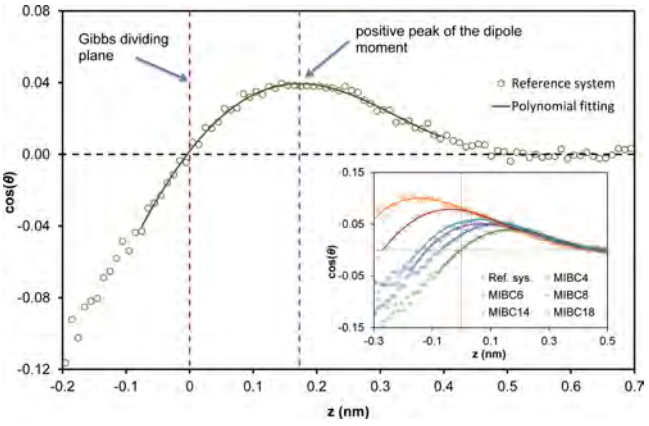

Figure 8. Limiting plane of the interface zone. The inset shows other fitting for 0, 4, 6, 8, 14, and 18 MIBCs.

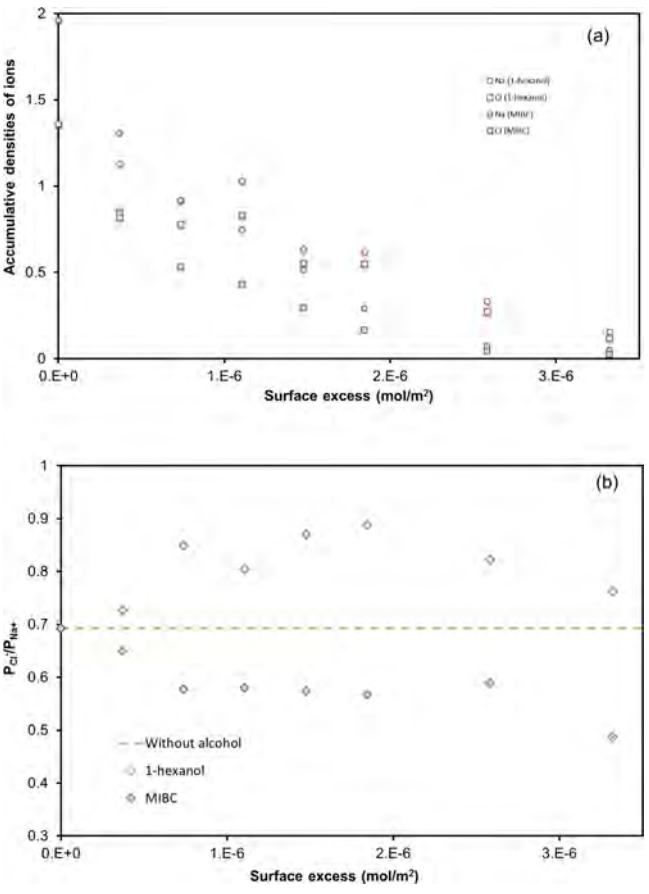

Figure 9. Densities of Na^+ and Cl^- within interfacial layer: absolute values (a) and anion/cation ratio (b).

space of ions and pushed both ions further inside the liquid phase. Figure 9b shows the anion/cation ratio for 1-hexanol solutions was higher than that in reference system (i.e., in the absence of alcohols). In contrast, the anion/cation ratio was lower at all MIBC concentrations. This means that though both ions were reduced by alcohol molecules, 1-hexanol relatively increased the presence of Cl^- over Na^+. Contrastingly, MIBC increased the presence of Na^+. The findings are consistent with an experimental study[8] where the adsorbed MIBCs and 1-hexanol had the opposite effects. It also confirms our initial assumption that the branching structure of MIBC enhances the presence of cations over anions.

DISCUSSION

The simulations showed that the rearrangement of water by alcohols can be used to qualitatively describe the surface potentials.[8] The disturbance of water and ions at the air/water interface was described clearly by the change in the dipole moment. The pre-existing two-layer arrangement of water was disrupted in a gradual manner with the increasing alcohol concentration. The hypothesis on the limit of the interfacial layer worked very well: it effectively described the contrasting effects of MIBC and 1-hexanol. The results indicate that the ionic state of the interfacial zone, rather than the surface tension,[10,11] might be the underpinning mechanism for MIBC selectivity in the flotation processes. In addition to the particle attachment, the ionic state of the interfacial zone also plays an important role in the dewetting kinetics of the contact line,[35] which is critical for particle detachment.

It is important to note that existence of the second water layer, which corresponding to a transition from the outmost water layer to bulk, has been confirmed experimentally.[34] However, the role this layer has on the properties of the interface is not understood. The simulations, in combination with previous experimental results, highlighted the significant role of the second layer. The usage of the dipole moment also demonstrated the critical role of disrupted/reoriented water molecules by the adsorbed alcohols. This factor has been inherently ignored by the conventional theoretical analysis, which relies on the interfacial quantities only.[36] On the other hand, the arrangement of water shows complicated behaviors with the adsorbed molecules.[37]

The relative adsorption between cation and anion at the air/water interface is a well-known problem in the literature.[38] It is well-accepted that the sizes of cation and anion have a profound impact on the surface layer.[39] Similarly, Na^+ has a stronger influence on MIBC adsorption than K^+.[40] The interaction between 1-butanol, K^+, and I^- can significantly alter the ion enhancement at the surface.[41] The selective impact can only be verified by molecular dynamics.[38] Yet the exact mechanism remains elusive. Recently, it has been shown that water plays a critical role in the ion−ion interactions with interfacial zone.[24] We also revealed the importance of water arrangement on a synergistic adsorption of surfactants.[32] As a result, the usage of water orientation in this study can capture the overall interaction of all species and water surface molecules.

CONCLUSION

The study applied molecular dynamics to describe the systems of MIBC/1-hexanol in NaCl solutions. The simulations quantified the density distribution of the adsorbed molecules, the change in surface tension and potential, and the water orientation. The water dipole moment profile was successfully applied to describe the contrasting ionic states of the interfacial zone between MIBC and 1-hexanol, as observed experimentally.

The new insights demonstrated the capacity of molecular dynamics to quantify the relative influences of adsorbed molecules. In particular, the method can be applied to predict the impact of frother structure with different electrolyte solutions, which can provide important information for the chemical design in mineral flotation.

DOI: 10.1021/la504471q
Langmuir 2015, 31, 50−56

The results also confirmed that the changes of ionic state of interfacial zone can be determined by the arrangement between alcohol and water. Such a factor is conveniently neglected by the conventional studies and needs to be included to correctly predict interfacial phenomena. The proposed role of the second water layer provides an important foundation for further studies.

AUTHOR INFORMATION

Corresponding Author

*E-mail c.phan@curtin.edu.au (C.M.P.).

Notes

The authors declare no competing financial interest.

ACKNOWLEDGMENTS

The work was supported by iVEC through the use of advanced computing resources. C. Nguyen was supported by the 322 scholarship, Ministry of Education and Training (Vietnam).

REFERENCES

(1) Klimpel, R. R.; Isherwood, S. Some industrial implications of changing frother chemical structure. *Int. J. Miner. Process.* **1991**, *33*, 369−381.

(2) Jun, Y.-D.; Kim, K. J.; Kennedy, J. M. Dynamic surface tension of heat transfer additives suitable for use in steam condensers and absorbers. *Int. J. Refrig.* **2010**, *33*, 428−434.

(3) Karakashev, S. I.; Nguyen, A. V.; Manev, E. D. A novel technique for improving interferometric determination of emulsion film thickness by digital filtration. *J. Colloid Interface Sci.* **2007**, *306*, 449−453.

(4) Nakahara, H.; Shibata, O.; Moroi, Y. Examination of surface adsorption of cetyltrimethylammonium bromide and sodium dodecyl sulfate. *J. Phys. Chem. B* **2011**, *115*, 9077−9086.

(5) Wang, L.; Yoon, R.-H. Effects of surface forces and film elasticity on foam stability. *Int. J. Miner. Process.* **2008**, *85*, 101−110.

(6) Nakahara, H.; Shibata, O.; Rusdi, M.; Moroi, Y. Examination of surface adsorption of soluble surfactants by surface potential measurement at the air/solution interface. *J. Phys. Chem. C* **2008**, *112*, 6398−6403.

(7) Warszyński, P.; Barzyk, W.; Lunkenheimer, K.; Fruhner, H. Surface tension and surface potential of Na n-dodecyl sulfate at the air−solution interface: Model and experiment. *J. Phys. Chem. B* **1998**, *102*, 10948−10957.

(8) Nguyen, C. V.; Phan, C. M.; Ang, H. M.; Nakahara, H.; Shibata, O.; Moroi, Y. Surface potential of 1-hexanol solution: Comparison with methyl isobutyl carbinol. *J. Phys. Chem. B* **2013**, *117*, 7615−7620.

(9) Phan, C. M.; Nakahara, H.; Shibata, O.; Moroi, Y.; Le, T. N.; Ang, H. M. Surface potential of methyl isobutyl carbinol adsorption layer at the air/water interface. *J. Phys. Chem. B* **2012**, *116*, 980−986.

(10) Comley, B. A.; Harris, P. J.; Bradshaw, D. J.; Harris, M. C. Frother characterisation using dynamic surface tension measurements. *Int. J. Miner. Process.* **2002**, *64*, 81−100.

(11) Le, T. N.; Phan, C. M.; Ang, H. M. Influence of hydrophobic tail on the adsorption of isomeric alcohols at air/water interface. *Asia Pac. J. Chem. Eng.* **2012**, *7*, 250−255.

(12) Chen, F.; Smith, P. E. Simulated surface tensions of common water models. *J. Chem. Phys.* **2007**, *126*.

(13) Yuet, P. K.; Blankschtein, D. Molecular dynamics simulation study of water surfaces: Comparison of flexible water models. *J. Phys. Chem. B* **2010**, *114*, 13786−13795.

(14) Mountain, R. D. An internally consistent method for the molecular dynamics simulation of the surface tension: Application to some TIP4P-type models of water. *J. Phys. Chem. B* **2009**, *113*, 482−486.

(15) Vega, C.; de Miguel, E. Surface tension of the most popular models of water by using the test-area simulation method. *J. Chem. Phys.* **2007**, *126*.

(16) Barnes, G.; Gentle, I. *Interfacial Science*; Oxford University Press: Oxford, UK, 2005.

(17) Hess, B.; Kutzner, C.; van der Spoel, D.; Lindahl, E. GROMACS 4: Algorithms for highly efficient, load-balanced, and scalable molecular simulation. *J. Chem. Theory Comput.* **2008**, *4*, 435−447.

(18) Schuttelkopf, A. W. PRODRG: a tool for high-throughput crystallography of protein-ligand complexes. *Acta Crystallogr., Sect. D* **2004**, *60*, 1355.

(19) Scott, W. R. P.; Hünenberger, P. H.; Tironi, I. G.; Mark, A. E.; Billeter, S. R.; Fennen, J.; Torda, A. E.; Huber, T.; Krüger, P.; van Gunsteren, W. F. The GROMOS biomolecular simulation program package. *J. Phys. Chem. A* **1999**, *103*, 3596−3607.

(20) Hermans, J.; Berendsen, H. J. C.; Van Gunsteren, W. F.; Postma, J. P. M. A consistent empirical potential for water−protein interactions. *Biopolymers* **1984**, *23*, 1513−1518.

(21) Jorgensen, W. L. Optimized intermolecular potential functions for liquid alcohols. *J. Phys. Chem.* **1986**, *90*, 1276−1284.

(22) Wardle, K. E.; Carlson, E.; Henderson, D.; Rowley, R. L. Molecular-dynamics simulation of the effect of ions on a liquid-liquid interface for a partially miscible mixture. *J. Chem. Phys.* **2004**, *120*, 7681−7688.

(23) Evans, D. J. The Nose−Hoover thermostat. *J. Chem. Phys.* **1985**, *83*, 4069.

(24) Venkateshwaran, V.; Vembanur, S.; Garde, S. Water-mediated ion−ion interactions are enhanced at the water vapor−liquid interface. *Proc. Natl. Acad. Sci. U. S. A.* **2014**, *111*, 8729−8734.

(25) Jungwirth, P.; Tobias, D. J. Specific ion effects at the air/water interface. *Chem. Rev.* **2006**, *106*, 1259−1281.

(26) Hess, B.; Bekker, H.; Berendsen, H. J. C.; Fraaije, J. G. E. M. LINCS: A linear constraint solver for molecular simulations. *J. Comput. Chem.* **1997**, *18*, 1463−1472.

(27) Deserno, M.; Holm, C. How to mesh up Ewald sums (II): An accurate error estimate for the P3M algorithm. arXiv preprint cond-mat/9807100, 1998.

(28) van der Spoel, D.; Lindahl, E.; Hess, B.; van Buuren, A.; Apol, E.; Meulenhoff, P.; Tieleman, D.; Sijbers, A.; Feenstra, K.; van Drunen, R. Gromacs User Manual version 4.5. 4, 2010.

(29) Senapati, S.; Berkowitz, M. L. Computer simulation study of the interface width of the liquid/liquid interface. *Phys. Rev. Lett.* **2001**, *87*, 176101.

(30) Vega, C.; de Miguel, E. Surface tension of the most popular models of water by using the test-area simulation method. *J. Chem. Phys.* **2007**, *126*, 154707−10.

(31) Tang, X.; Huston, K. J.; Larson, R. G. Molecular dynamics simulations of structure−property relationships of Tween 80 surfactants in water and at interfaces. *J. Phys. Chem. B* **2014**, *118*, 12907−12918.

(32) Phan, C. M.; Nguyen, C. V.; Yusa, S.-i.; Yamada, N. L. Synergistic adsorption of MIBC/CTAB mixture at the air/water interface and applicability of Gibbs adsorption equation. *Langmuir* **2014**, *30*, 5790−5796.

(33) Kathmann, S. M.; Kuo, I. F. W.; Mundy, C. J. Electronic effects on the surface potential at the vapor−liquid interface of water. *J. Am. Chem. Soc.* **2008**, *130*, 16556−16561.

(34) Fan, Y.; Chen, X.; Yang, L.; Cremer, P. S.; Gao, Y. Q. On the structure of water at the aqueous/air interface. *J. Phys. Chem. B* **2009**, *113*, 11672−11679.

(35) Phan, C. M.; Nguyen, A. V.; Evans, G. M. Assessment of hydrodynamic and molecular-kinetic models applied to the motion of the dewetting contact line between a small bubble and a solid surface. *Langmuir* **2003**, *19*, 6796−6801.

(36) Prosser, A. J.; Franses, E. I. Adsorption and surface tension of ionic surfactants at the air-water interface: Review and evaluation of equilibrium models. *Colloids Surf., A* **2001**, *178*, 1−40.

(37) Allen, H. C.; Casillas-Ituarte, N. N.; Sierra-Hernández, M. R.; Chen, X.; Tang, C. Y. Shedding light on water structure at air-aqueous interfaces: Ions, lipids, and hydration. *Phys. Chem. Chem. Phys.* **2009**, *11*, 5538−5549.

DOI: 10.1021/la504471q
Langmuir 2015, 31, 50−56

(38) Garrett, B. C. Ions at the air/water interface. *Science* **2004**, *303*, 1146−1147.
(39) Boström, M.; Kunz, W.; Ninham, B. W. Hofmeister effects in surface tension of aqueous electrolyte solution. *Langmuir* **2005**, *21*, 2619−2623.
(40) Ozdemir, O.; Karakashev, S. I.; Nguyen, A. V.; Miller, J. D. Adsorption and surface tension analysis of concentrated alkali halide brine solutions. *Miner. Eng.* **2009**, *22*, 263−271.
(41) Krisch, M. J.; D'Auria, R.; Brown, M. A.; Tobias, D. J.; Hemminger, C.; Ammann, M.; Starr, D. E.; Bluhm, H. The effect of an organic surfactant on the liquid−vapor interface of an electrolyte solution. *J. Phys. Chem. C* **2007**, *111*, 13497−13509.

DOI: 10.1021/la504471q
Langmuir 2015, 31, 50−56